

Development of solid microneedles for transdermal drug delivery in companion animals



A. Muftić*, Z. Imamović, M. Bisić, J. Šupić, A. Alić and E. Muftić

Abstract

The objective of this paper was to create an economical and abecedarian 3D printing method for the production of solid microneedles, as a more efficient transdermal drug delivery method, for day-to-day use in companion animals. The process of 3D printing was conducted using two types of 3D printers, utilizing the FDM and SLA printing techniques. Modulus of Elasticity was calculated for the determination of mechanical properties of the material, where the printed specimen was subjected to axial loading, and deformations were measured using an optical scanner. Post-processing was conducted by washing microneedles in isopropyl alcohol, followed by UV curing. The procedure of testing penetration capabilities was conducted at two sites of cat skin: *Auris externa* and the lateral part of the abdomen. The SLA printing

method was more precise, resulting in higher quality microneedles for animal use compared to the FDM printing technique. Modulus of Elasticity was calculated and the value $E=0.9$ GPa can be used. Testing proved that the printed model was able to penetrate the skin at the tested sites. The use of microneedles is simple and economical, and therefore has wide applications in small animal practice. Veterinarians can access microneedle design repositories and print them for more effective transdermal drug delivery. The multifunctionality and transferability of the design in the present study ensure that it can be further modified to provide personalized therapy.

Key words: 3D printing; microneedle; transdermal drug delivery; companion animals

Introduction

Avoidance of emotional stress and needle-caused injuries associated with the usual treatment of animals, while

improving animal compliance during veterinary procedures should be one of the main goals of animal welfare. These

Abdullah MUFTIĆ, DVM, Senior Assistant, (Corresponding author, e-mail: abdullah.muftic@vfs.unsa.ba), University of Sarajevo – Veterinary Faculty, Sarajevo, Bosnia and Herzegovina; Zejd IMAMOVIĆ, MSc Mechanical Engineering, Senior Assistant, University of Sarajevo – Faculty of Mechanical Engineering, Sarajevo, Bosnia and Herzegovina; Muhamed BISIĆ, BSc, Mechanical Engineering, Student, University of Sarajevo – Faculty of Mechanical Engineering, Sarajevo, Bosnia and Herzegovina; Jovana ŠUPIĆ, DVM, Senior Assistant, University of Sarajevo – Veterinary Faculty, Sarajevo, Bosnia and Herzegovina; Amer ALIĆ, DVM, PhD, Associate Professor, University of Sarajevo – Faculty of Veterinary Faculty, Sarajevo, Bosnia and Herzegovina; Emina MUFTIĆ, DVM, Senior Assistant, University of Sarajevo – Faculty of Pharmacy, Sarajevo, Bosnia and Herzegovina

objectives could be fulfilled by achieving easier methods of medication administration, such as cutaneous delivery. Several methods for transdermal drug delivery have been developed, though most have had limited success due to the problems regarding the transfer of high molecular weight compounds across the skin (Langer, 2004). Microneedles (MNs) are novel, microscopic-size applicators used for medical treatments. Several studies have emphasized the advantages of using MNs, as they are a less painful and more efficient way of transdermal drug delivery (Teo et al., 2006; Indermun et al., 2014). MNs facilitate drug diffusion by piercing microscale pores in the *stratum corneum*, while not affecting nociceptors in the skin, thus eliminating or minimizing pain. Additionally, MNs reduce the required doses and improve the bioavailability of used medicines by avoiding the degradation of drugs in the gastrointestinal tract, which reduces plasma level oscillations often caused by other types of treatments (Teo et al., 2004; Papich and Narayan, 2022). Most studies on MNs to date have focused on human use of the product and are executed regarding the composition and thickness of human skin. Animal skin, predominantly the *epidermis*, is substantially thinner (Schwarz et al., 1979; Noli and Colombo, 2020), thus making human-focused MNs inconvenient for use in animals. However, MN manufacturing is not an easy process, since it demands the usage of specialized equipment capable of producing needles of microscopic scale.

Nowadays, MNs are mainly produced using 3d printing techniques (Dabbagh et al., 2021). A microneedle array (MNA) is composed of single or multiple individual MNs on a flat base (substrate). The selection of the 3d printing technique is based on several factors, including the size and design of MNs, printing material (resin

and filaments), and the required finish quality of the product (Dabbagh et al., 2021). While Composite Extrusion Modelling (CEM) and Filament Metal Printing (FMP) are 3d printing techniques for the production of multiuse MNAs, Fused Deposition Modelling (FDM), Selective Laser Sintering (SLS), and Stereolithography (SLA) are mainly used for the production of expendable MNAs (Economidou and Douroumis, 2021). SLA 3d printers belong to a family of additive manufacturing technologies known as vat-photopolymerization, commonly known as resin 3d printing. These machines are all built around the same principle, using a light source – a laser or projector – to cure liquid resin into hardened plastic. SLA 3d printers use light-reactive thermoset materials (resin). When SLA resins are exposed to certain wavelengths of light, short molecular chains join together, polymerizing monomers and oligomers into solidified rigid or flexible geometries (Ma, 2013). A possible drawback regarding the production of MNs and MNAs is the high cost, mainly due to significant power consumption by 3d printers, and the price of printing materials. In addition, the selection of 3d printing material is another issue since the selected material has to comply with basic principles of structural integrity when inserted into the animal skin.

There are insufficient data about mechanical properties such as the Modulus of Elasticity, which is essential regarding the safety of using devices made from this material in veterinary medicine. Modulus of Elasticity is the measurement of a material's resistance to deformation when stress is applied (Askeland, 1996). The Modulus of Elasticity of polymer pieces obtained by 3d printing depends on the material and printing techniques (layer thickness, printing precision, etc.).

There are several options regarding the design and structure of MNs, including solid, hollow, and intradermal-soluble designs that are suitable for different purposes. Solid MNs are the most versatile of the aforementioned since they allow the implementation of the poke-and-patch method, either with or without drug coating (Quinn et al., 2014). The poke-and-patch method consists of the use of MNs to penetrate the *stratum corneum* while creating micropores. This method substantially improves topical drug delivery since the main defensive barrier of the skin is disrupted (Gupta et al., 2011).

This study aimed to create an economical and abecedarian 3d printing method for the production of solid MNAs using inexpensive and harmless printing materials and SLA printing techniques for day-to-day use in transdermal drug delivery in companion animals. This study also aimed to determine the Modulus of Elasticity of the selected material to act by the “Do no harm” principle of veterinary medicine.

Materials and methods

The methods applied in the present study are divided into three subcatego-

ries due to the specificity of each process.

Process of 3d printing

Two types of 3d printers were used based on the FDM and SLA printing techniques. FDM 3d printers work by extruding thermoplastic filaments through a heated nozzle, melting the material, and applying the plastic layer by layer to a build platform. For the test, Ultimaker S5 Pro (Ultimaker®, The Netherlands) with a 0.4 mm nozzle was used with PLA filament and maximum quality profile. The SLA 3d printer used in this project was Anycubic Photon Mono X (Anycubic®, China).

Computer-aided design (CAD) of MNs has a height of 2 mm, and 0.5 mm since plastic shrinkage was expected. In the present study, the slicer Chitubox V1.9.0 (CBD-Tech®, China) was used. The model of MNs was designed to have 12 rows of 12 needles per row (144 MNs) placed on a 200 mm plate that serves as a substrate (Figure 1). A fully designed model from CAD software was saved as an .stl extension and was accessed by the software used for preparing CAD files for 3d printing (slicer).

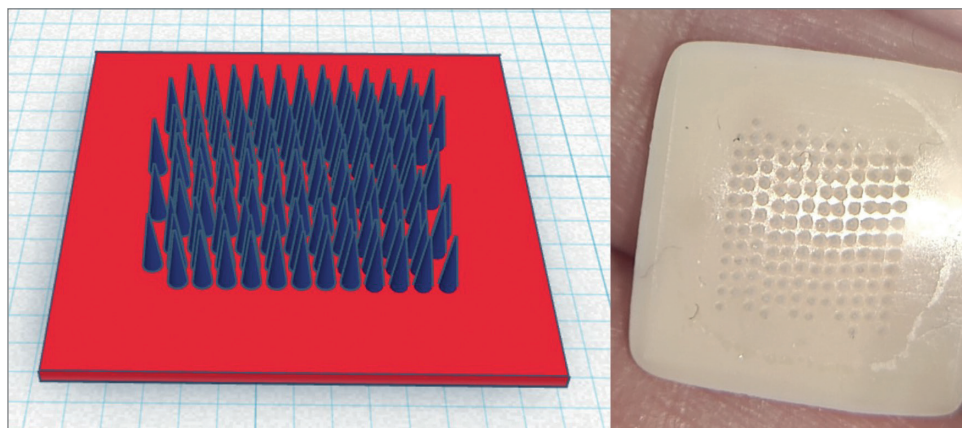


Figure 1. a) Design of microneedles for 3D printing; b) 3D printed microneedles

The parameters set for the 3d printing of MNs were:

- Layer height: 0.025 mm
- Bottom layer count: 4
- Exposure Time: 1.1 s
- Bottom Exposure Time: 40 s
- Lifting speed: 180 mm/min
- Retract speed: 240 mm/min

Post-processing was conducted by washing MNAs in isopropyl alcohol for 20 minutes, followed by UV curing for 20 minutes.

The finished design product in both .stl and .pwm extension is available in the GitHub repository (GitHub, 2021).

Determination of mechanical properties

The material used for 3d printing was Anycubic UV 405 nm 3d Resin (Anycubic®, China). Due to the need to obtain the Modulus of Elasticity for the used material, the experimental method was used, where the printed specimen was subjected to axial loading, and deforma-

tions were measured via an optical scanner ATOS Core (Atos®, France). ATOS Core specializes in 3d scanning of small and medium objects up to 200 x 150 x 150 mm. This device, in addition to 3d scanning of body shapes of correct and incorrect geometry, allows the measurement of deformations, displacements, displacement speeds, etc. After scanning, the file was opened in a compatible Generic Object Model (GOM) software solution in which it was possible to analyse the deformations of the recorded object. After 3d printing, the specimen had the following initial dimensions:

$L_0 = 83 \text{ mm}$ – length

$t = 20.5 \text{ mm}$ – thickness

$b = 50.2 \text{ mm}$ – width

The cross-sectional area of the specimen was:

$$A = b \cdot t = 1029 \text{ mm}^2$$

For the optical scanner to recognize points on the loaded specimen, the scan-



Figure 2. Specimen subjected to axial load with software recognition and determination of reference points on the surface

ning area needed to be prepared – painted in white, with many black points (Figure 2). Such contrast was sufficient for the scanner to discern points and measure their relative deformations (Kljuno et al., 2021a; Yadav et al., 2021).

During the experiment, a clamp was used together with an electric sensor where the battery input voltage (U) was 12.8 V and the response was defined by the constant k:

$$k = 15000 \text{ kg} \cdot \frac{1 \text{ V}}{2 \text{ mV}}$$

Each phase was recorded with the ATOS Core scanner during the loading process. After scanning, files were processed in GOM Correlate Inspect (Carl Zeiss AG®, Germany) numerical software and relative deformation in the x-axis ε_x was observed.

Determination of the Modulus of Elasticity was conducted by calculating several physical measures. The compressive force of the clamp depends on the encoder output voltage and was determined from the next relation:

$$F(U_o) = -k \cdot \frac{U_i}{U} \cdot g$$

$$N = -15000 \text{ kg} \frac{1 \text{ V}}{2 \text{ mV}} \cdot \frac{U_o}{12.8 \text{ V}} \cdot 9.81 \frac{\text{m}}{\text{s}^2} =$$

$$= -5748 \cdot U_i \frac{\text{N}}{\text{mV}},$$

where U_o [mV] is an output voltage through the phase (i = 1,2,3...) of amplifying axial loading.

At phase i = 7 output voltage measured $U_7 = 2.04 \text{ mV}$, therefore compressive force at this phase was:

$$F = F(U_7) = -5748 \cdot 2.04 \text{ mV}$$

$$\frac{N}{\text{mV}} = -11 \ 726 \text{ N}$$

At this phase, the absolute deformation of the specimen (ΔL) was calculated by taking the difference between measured lengths of the clamp at phases i = 7 and i = 2. At phase i = 2 clearance between the specimen and clamp jaws was zero. Also, local kneading of the moving jaw of a clamp into the polymer needed to be considered to obtain the correct result. After inspecting, this local kneading (was approximately (δ_{lk}). Finally, absolute deformation was:

$$\Delta L = L_{s7} - L_{s2} + \delta_{lk} =$$

$$= 96.1 - 97.64 + 0.4 \text{ mm} =$$

$$= -1.14 \text{ mm}$$

Knowing the absolute deformation and initial length of the specimen, relative deformation in the axial (x) axis was analytically determined as:

$$\varepsilon_x^{ana} = \frac{\Delta L}{L_0} = \frac{-1.14 \text{ mm}}{83 \text{ mm}} =$$

$$= -0.0137 = -1.37 \%$$

Using the results from the software, we can obtain a value of relative deformation for phase , the same phase where analytical approaches were used. Due to the dispersion of the results of relative deformation at different points, a set of a large number of points (n=17) was taken into consideration (Figure 3).

Using the simple average value method, the experimental relative deformation of the polymer specimen in the load phase i = 7 was:

$$\varepsilon_x^{exp} = \frac{\sum \varepsilon_{xi}}{n} = -1.2 \%$$

By obtaining the relative deformation of the polymer specimen, it was possible to determine the Modulus of Elasticity (Goodier and Timoshenko, 1970; Rees, 2016).

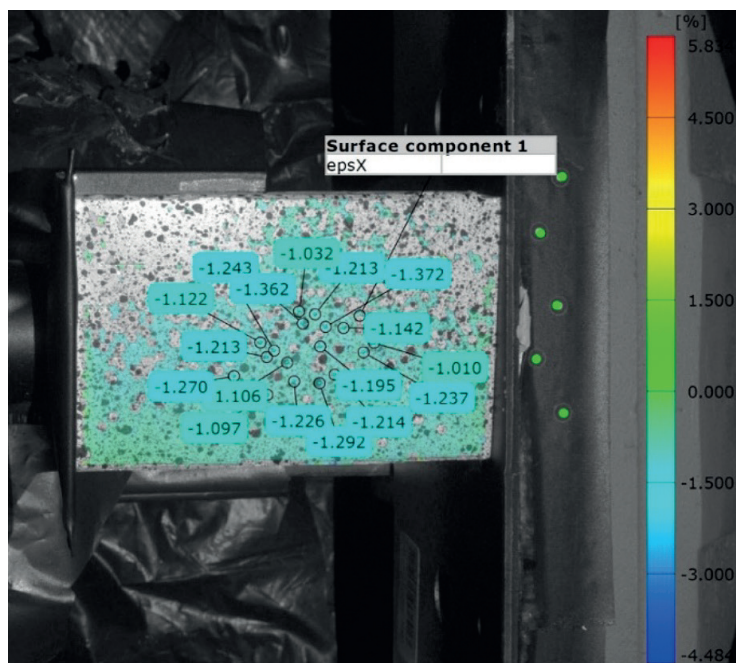


Figure 3.
Relative
deformation in
the x-axis at the
recognised points

Testing of MNAs

The skin of a cat that recently perished from collision with a vehicle was used as the biological model for MN testing. Testing was conducted at the Laboratory for Pathology. The procedure of testing MN penetration capabilities was conducted at two sites: the *Auris externa*, selected since the skin is thinnest on this part of the animal body, and the lateral part of the abdomen where adipose tissue is mainly located (Noli and Colombo, 2020). At both of testing sites, the skin was intact.

Simple visualization was conducted to observe whether MNs successfully penetrated the skin. Subsequently, puncture sites were observed by the Z4 Zoom Stereoscope (LW Scientific®, USA).

For the poke-and-patch test, the procedure of MN application was conducted by pressing the device onto the skin with the thumb and removing it after 5 seconds. MNs applied to the *Auris externa* were

removed instantly post-application, and MNs on the lateral part of the abdomen were left inserted for 5 minutes to observe differences in application methods.

Results

Printing process, analytical and experimental determination of the Modulus of Elasticity of MNA material

The FDM printing method provided inadequate quality of MNs which had unsatisfactory shape and form, and did not achieve the desired precision for animal use. The SLA printing method was more precise, resulting in MNs of higher quality for animal use (Figure 1). Furthermore, the number of MNAs varied greatly between the two tested methods for a similar printing time. The duration of the SLA printing method was 15 minutes, which was 3 minutes slower compared

to FDM printing. However, when using SLA 3d printers, 50 MNAs were printed simultaneously in 15 minutes, compared to using FDM printers where the total printing time was 600 minutes (12 minutes for each of the 50 MNAs individually).

The measured mean size (\bar{x}) of MNs post-printing was 481 μm (441–512 μm), with MNs longer at the border of the substrate ($\bar{x} = 497 \mu\text{m}$) than in the centre ($\bar{x} = 463 \mu\text{m}$). Exposure to UV light triggers the formation of additional chemical bonds within the 3d-printed part, making the material stronger and stiffer in the process. Furthermore, the curing process transforms MNs into non-toxic and safe objects, which is a requirement when using MNs on animal skin.

Using Hooke's Law $\sigma = E \cdot \epsilon_x$ and relation for the normal stress in the axially loaded bar $\sigma = F/A$, with the analytically obtained value of relative deformation ϵ_x^{ana} , the Modulus of Elasticity in the printed specimen was calculated:

$$\begin{aligned} E^{exp} &= \frac{\sigma}{\epsilon_x^{exp}} = \frac{F}{A \cdot \epsilon_x^{exp}} = \\ &= \frac{-11726 \text{ N}}{1029 \text{ mm}^2 \cdot (-0.012)} = \\ &= 950 \text{ MPa} = 0.95 \text{ GPa} \end{aligned}$$

Using the Hooke's relation and equal stress exposure in the analytical approach, the Modulus of Elasticity of the resin, with the experimentally obtained Value of Relative Deformation ϵ_x^{exp} using a 3d scanner was determined:

$$\begin{aligned} E^{ana} &= \frac{F}{A \cdot \epsilon_x^{ana}} = \\ &= \frac{-11726 \text{ N}}{1029 \text{ mm}^2 \cdot (-0.0137)} = \\ &= 832 \text{ MPa} = 0.83 \text{ GPa} \end{aligned}$$

The approximate value between these two for the given material of MNs, can be used.

Testing of MNAs

Testing of MNs showed that the printed model was able to penetrate the skin at the *Auris externa* (Figure 4), and on the lateral part of the abdomen. It is concluded that the pressure required for puncturing is not greater than the pressure exercised by a thumb.



Figure 4. Application of microneedles to the *Auris externa* of a cat

Differences between application sites were not observed. Changes between punctures in the skin were not observed whether MNs were removed instantly post-application, or left inserted for 10 minutes.

Discussion

The literature highlighting the importance of 3d printed MNs has grown rapidly in recent years for human medicine (Dabbagh et al., 2021). The advantage of MNs is that they are well tolerated and less painful than traditional hypodermic needles (Banks et al., 2011). The utilization of the poke-and-patch method of MNs application is the most common one. Its simplicity, from a technical viewpoint, makes it attractive for clinical use (Guillot et al., 2020). A study conducted in 2011 on MNs pre-treatment followed by application of a transdermal naltrexone patch led to higher naltrexone plasma levels in healthy human subjects compared to traditional patch application (Banks et al., 2011). These findings are not the exception since the majority of research has accentuated the improvement in the bioavailability of vitamins (Kim et al., 2018), hormones (Resnik et al., 2018), antibiotics (Risbud and Bhonde, 2000), therapeutic proteins (Cheung et al., 2015), and natural compounds (Paleco et al., 2014) during the poke-and-patch method in human medicine. Furthermore, since topical medication is widely used in both human (Bewley, 2008; Mooney et al., 2015) and veterinary medicine (Breen and Johnson, 1977), MNAs should reduce dosage while providing a similar or better effect in animal healthcare.

Since animal skin has a substantially thinner epidermis (Schwarz et al., 1979; Noli and Colombo, 2020) and the nociceptors are closer to the skin surface,

the MNs designed for human use could prove inadequate due to the possible pain of application of MNs inflicted on the animal. Unfortunately, MNs and MNAs have not had the same popularity in veterinary medicine, with only several papers published regarding their uses. To the best of our knowledge, there are no studies regarding the design of solid MNs and MNAs for use in companion animals. Research within the scope of veterinary medicine have not provided a design for the most versatile type of MNs – solid MNs but have instead been focused on the effects of dissolvable (Arya et al., 2016) and insertion-responsive (Choi et al., 2020) MNs in immunoprophylaxis of animals. Based on our research, the SLA printing technique is a better choice for solid MNAs for animal use since the sizes are microscopic and precision is often problematic. The SLA printing technique provided better precision and quality of the finished product compared to FDM. To create an adequate design of solid MNs, certain physical properties of the used material had to be met. The Modulus of elasticity and relative deformation are the most important mechanical properties of a material (Goodier and Timoshenko, 1970). For 3d printed MNs and MNAs, these physical properties can be determined either by experiment - using an optical scanner, or by using the analytical approach (Kljuno et al., 2021b). The similarity of results obtained by analytical and experimental methods allows employing either of them in material testing for future MNs designs and different MNs application procedures. Due to the simplicity of the experimental method, and the similarity of results comparing the two methods, avoiding the analytical method and testing only via an optical scanner should prove adequate.

Knowing the value of the Modulus of Elasticity allows numerical analysis of the load, *i.e.*, strength, and stability of MNs made from biocompatible materials that would be applied as a final product. Regardless, it would be necessary to determine the toughness of animal skin to create MNs of reciprocal characteristics for safe application without substantial deformation occurrence. To the best of our knowledge, fundamental studies determining the physical properties of animal skin are yet to be conducted.

With the virtue of this research, future changes could be made by taking these findings into account. Further research on the use of solid MNs would include an accurate assessment of animal skin penetration using histological methods and animal models. The multifunctionality and transferability of the design in the present study ensure that it can be further modified to provide personalised therapy. If the need arises in the production of hollow or coated MNs, this design will prove useful as a starting point for future alterations.

References

1. ARYA, J. M., K. DEWITT, M. SCOTT-GARRARD, Y. W. CHIANG and M. R., PRAUSNITZ (2016): Rabies vaccination in dogs using a dissolving microneedle patch. *J. Control. Release* 239, 19-26. 10.1016/j.jconrel.2016.08.012
2. ASKELAND, D. R. (1996): Introduction to materials. In: Askeland, D. R., P. P. Fulay and W. J. Wright: The science and engineering of materials. Springer (2-17).
3. BANKS, S. L., K. S. PAUDEL, N. K. BROGDEN, C. D. LOFTIN and A. L. STINCHCOMB (2011): Diclofenac enables prolonged delivery of naltrexone through microneedle-treated skin. *Pharm. Res.* 28, 1211-1219. 10.1007/s11095-011-0372-2
4. BEWLEY, A. (2008): Dermatology Working Group. Expert consensus: time for a change in the way we advise our patients to use topical corticosteroids. *Br. J. Dermatol. Suppl.* 158, 917-920. 10.1111/j.1365-2133.2008.08479.x
5. GitHub (2021): 3D STL Design of microneedles with sliced .pwm file for SLA 3D printing <https://github.com/bisk3/MNs?fbclid=IwAR13tHCVZNH-3Tzxo0kzBjSpPkpXQ6QcuVvuPHbRNQBfTxXwbN-yYMhgsU> [Accessed March 21st, 2023].
6. BREEN, P. T. and G. L. JOHNSON (1977): Epidermal atrophy [in a dog] caused by excessive use of a topical corticosteroid: a case report. *J. Am. Anim. Hosp. Assoc.* 13, 713-715.
7. CHEUNG, K., G. WEST and D. B. DAS (2015): Delivery of large molecular protein using flat and short microneedles prepared using a focused ion beam (FIB) as a skin ablation tool. *Drug Deliv. Transl. Res.* 5, 462-467. 10.1007/s13346-015-0252-0
8. CHOI, I. J., W. NA, A. KANG, M. H. AHN, M. YEOM, H. O. KIM, J. W. LIM, S. O. CHOI, S. K. BAEK, D. SONG and J. H. PARK (2020): Patchless administration of canine influenza vaccine on dog's ear using insertion-responsive microneedles (IRMN) without removal of hair and its in vivo efficacy evaluation. *Eur. J. Pharm. Biopharm.* 153, 150-157. 10.1016/j.ejpb.2020.06.006
9. DABBAGH, S. R., M. R. SARABI, R. RAHBARGHAZI, E. SOKULLU, A. K. YETISEN and S. TASOGLU (2021): 3d-printed microneedles in biomedical applications. *iScience* 24, 102012. 10.1016/j.isci.2020.102012
10. ECONOMIDOU, S. N. and D. DOUROUMIS (2021): 3d printing as a transformative tool for microneedle systems: Recent advances, manufacturing considerations and market potential. *Adv. Drug Deliv. Rev.* 173, 60-69. 10.1016/j.addr.2021.03.007
11. GOODIER, J. N. and S. TIMOSHENKO (1970): Theory of elasticity. McGraw-Hill.
12. GUILLOT, A. J., A. S. CORDEIRO, R. F. DONNELLY, M. C. MONTESINOS, T. M. GARRIGUES and A. MELERO (2020): Microneedle-based delivery: an overview of current applications and trends. *Pharmaceutics* 12, 569. 10.3390/pharmaceutics12060569
13. GUPTA, J., H. S. GILL, S. N. ANDREWS and M. R. PRAUSNITZ (2011): Kinetics of skin resealing after insertion of microneedles in human subjects. *J. Control. Release.* 154, 148-155. 10.1016/j.jconrel.2011.05.021
14. INDERMUN, S., R. LUTTGE, Y. E. CHOONARA, P. KUMAR, L. C. DU TOIT, G. MODI and V. PILLAY (2014): Current advances in the fabrication of microneedles for transdermal delivery. *J. Control. Release.* 185, 130-138. 10.1016/j.jconrel.2014.04.052
15. KIM, H. G., D. L. GATER and Y. C. KIM (2018): Development of transdermal vitamin D3 (VD3) delivery system using combinations of PLGA nanoparticles and microneedles. *Drug Deliv. Transl. Res.* 8, 281-290. 10.1007/s13346-017-0460-x
16. KLJUNO, E., F. RAZIC, A. CATOVIC and E. MESIC (2021): Deformation and stress analysis of a U-shaped pipe compensator using a 3d scanner. *Period. Eng. Nat. Sci.* 9, 830-841. 10.21533/pen.v9i2.1900

17. KLJUNO, E., F. RAZIC, E. MESIC and A. CATOVIC (2021): Structural stress and strain analysis using a 3d scanner. International Symposium on Innovative and Interdisciplinary Applications of Advanced Technologies. Springer, Cham (617-634).
18. LANGER, R. (2004): Transdermal drug delivery: past progress, current status, and future prospects. *Adv. Drug Deliv. Rev.* 56, 557-558. 10.1016/j.addr.2003.10.021
19. MA, X. L. (2013): Research on application of SLA technology in the 3d printing technology. *Appl. Mech. Mater.* 401, 938-941.
20. MOONEY, E., M. RADEMAKER, R. DAILEY, B. S. DANIEL, C. DRUMMOND, G. FISCHER, R. FOSTER, C. GRILLS, A. HALBERT, S. HILL and E. KING (2015): Adverse effects of topical corticosteroids in paediatric eczema: Australasian consensus statement. *Australas. J. Dermatol.* 56, 241-251. 10.1111/ajd.12313
21. NOLI, C. and S. COLOMBO (2020): *Feline Dermatology*. Springer Nature.
22. PALECO, R., S. R. VUCEN and A. M. CREAN (2014): Enhancement of the in vitro penetration of quercetin through pig skin by combined microneedles and lipid microparticles. *Int. J. Pharm.* 472, 206-213. 10.1016/j.ijpharm.2014.06.010
23. PAPICH, M. G. and R. J. NARAYAN (2022): Naloxone and nalmefene absorption delivered by hollow microneedles compared to intramuscular injection. *Drug Deliv. Transl. Res.* 12, 376-383. 10.1007/s13346-021-01096-0
24. QUINN, H. L., M. C. KEARNEY, A. J. COURTENAY, M. T. MCCRUDDEN and R. F. DONNELLY (2014): The role of microneedles for drug and vaccine delivery. *Expert Opin. Drug Deliv.* 11, 1769-1780. 10.1517/17425247.2014.938635
25. REES, D. W. (2016): *Mechanics of solids and structures*. World Scientific Publishing Company.
26. RESNIK, D., M. MOŽEK, B. PEČAR, A. JANEŽ, V. URBANČIČ, C. ILIESCU and D. VRTAČNIK (2018): In vivo experimental study of noninvasive insulin microinjection through hollow Si microneedle array. *Micromachines* 9, 40. 10.3390/mi9010040
27. RISBUD, M. V. and R. R. BHONDE (2000): Polyacrylamide-chitosan hydrogels: in vitro biocompatibility and sustained antibiotic release studies. *Drug Deliv.* 7, 69-75. 10.1080/107175400266623
28. SCHWARZ, R., J. M. W. LE ROUX, R. SCHALLER and K. NEURAND (1979): Micromorphology of the skin (epidermis, dermis, subcutis) of the dog. *Onderstepoort J. Vet. Res.* 46, 105-109. hdl.handle.net/2263/53794
29. TEO, A. L., C. SHEARWOOD, K. C. NG, J. LU and S. MOOCHHALA (2006): Transdermal microneedles for drug delivery applications. *Mater. Sci. Eng. B Solid State Mater. Adv. Technol.* 132, 151-154. 10.1016/j.mseb.2006.02.008
30. YADAV, P. R., M. N. MUNNI, L. CAMPBELL, G. MOSTOFA, L. DOBSON, M. SHITTU, S. K. PATTANAYEK, M. J. UDDIN and D. B. DAS (2021): Translation of polymeric microneedles for treatment of human diseases: Recent trends, Progress, and Challenges. *Pharmaceutics* 13, 1132. 10.3390/pharmaceutics13081132

Razvoj čvrstih mikroigala za transdermalnu aplikaciju lijekova u kućnih ljubimaca

Abdullah MUFTIĆ, dr. med. vet., viši asistent, Univerzitet u Sarajevu – Veterinarski fakultet, Sarajevo, Bosna i Hercegovina; Zejd IMAMOVIĆ, MSc mašinstva, viši asistent, Univerzitet u Sarajevu – Mašinski fakultet, Sarajevo, Bosna i Hercegovina; Muhamed BISIĆ, BSc mašinstva, student, Univerzitet u Sarajevu – Mašinski fakultet, Sarajevo, Bosna i Hercegovina; Jovana ŠUPIĆ, dr. med. vet., viši asistent, Univerzitet u Sarajevu – Veterinarski fakultet, Sarajevo, Bosna i Hercegovina; dr. sc. Amer ALIĆ, dr. med. vet., izvanredni profesor, Univerzitet u Sarajevu – Veterinarski fakultet, Sarajevo, Bosna i Hercegovina; Emina MUFTIĆ, dr. med. vet., viši asistent, Univerzitet u Sarajevu – Farmaceutski fakultet, Sarajevo, Bosna i Hercegovina

Cilj ovog rada je kreiranje ekonomične i abecedarne metode 3D printanja za proizvodnju čvrstih mikroigala, kao učinkovitije transdermalne metode aplikacije lijeka, za svakodnevnu uporabu u kućnih ljubimaca. Proces 3D printanja se provodi pomoću nekoliko tipova 3D printera, koristeći FDM i SLA tehnike printanja. Modul elasticiteta izračunat je za određivanje mehaničkih svojstava korištenog materijala, pri čemu je printani uzorak podvrgnut

aksijalnom opterećenju, a deformacije su mjerene optičkim skenerom. Naknadna obrada je obavljena ispiranjem MNA u izopropil alkoholu, nakon čega je uslijedilo UV sušenje. Procedura ispitivanja sposobnosti penetracije MNS provedena je na dva mjesta na koži mačke: *Auris externa* i lateralni dio abdomena. SLA metoda printanja bila je preciznija, što je rezultiralo mikroiglama veće kvalitete za uporabu na životinjama u usporedbi s FDM tehnikom

printanja. Modul elasticiteta je izračunat i može se koristiti vrijednost $E=0,9$ GPa. Testiranje printanih mikroigli je pokazalo da je model bio u stanju da penetrira u kožu na testiranim područjima. Uporaba mikroigli je jednostavna i ekonomična, stoga može biti široko rasprostranjena u praksi malih životinja. Veterinari mogu pristupiti repozitorijumi-

ma dizajna mikroigli i sami iste printati, kako bi ih koristili za učinkovitiju transdermalnu aplikaciju lijekova. Multifunkcionalnost i primjenjivost dizajna u ovoj studiji osiguravaju mogućnost daljnje modifikacije da bi se omogućila individualna terapija.

Ključne riječi: *3D printanje, mikroigle, transdermalna isporuka lijekova, kućni ljubimci*